

# Wake-induced long range repulsion of aqueous dunes: Supplementary Information

Karol A. Bacik,<sup>1,\*</sup> Sean Lovett,<sup>2,†</sup> Colm-cille P. Caulfield,<sup>3,1</sup> and Nathalie M. Vriend<sup>1,3</sup>

<sup>1</sup>*Department of Applied Mathematics & Theoretical Physics,  
University of Cambridge, Centre for Mathematical Sciences,  
Wilberforce Road, Cambridge CB3 0WA, United Kingdom*

<sup>2</sup>*Schlumberger Cambridge Research, High Cross, Madingley Rd, Cambridge CB3 0EL, United Kingdom*

<sup>3</sup>*BP Institute, University of Cambridge, Bullard Laboratories,  
Madingley Road, Cambridge CB3 0EZ, United Kingdom*

(Dated: September 12, 2019)

## FLOW PARAMETERS

At rest, the free surface of water is 42.4 cm above the bottom of the flume and the paddles are submerged at a depth of 6.6 cm. Different choices were made for the rotation rate of the table and paddle assembly, depending on the type of experiments. For the separation experiments, the rotation rate of the table is fixed at  $\Omega_{\text{table}} = -4.5$  rpm and the paddle assembly rotates in the opposite direction with angular speed  $\Omega_{\text{paddle}} = 8.5$  rpm, resulting in a total differential of  $\Omega_{\text{tot}} = 13$  rpm, where left-handed coordinate system should be understood. As the system is completely symmetric under direction reversal, for the sake of visual consistency, Fig. 1 and the insets of Fig. 3a are mirror reflections. Figure S1a shows the vertical profile of azimuthal velocity which is induced by the driving unit in an empty tank. Figures S1b and S1c show the velocity field in the presence of dunes in close proximity and dunes in the antipodal configuration. In all cases in the top layer the velocity field oscillates periodically as the paddles go by. In the absence of dunes the flow is temporally homogeneous in the bottom 20 cm of the tank (Fig. S1a), but the presence of dunes affects significantly the velocity profile (Fig. S1d). Each dune imposes substantial form drag which effectively decreases mean velocity in the bottom layer. This way dunes affect the velocity field up to about three dune heights from the ground, but the influence seems to be independent of the separation between dunes.

For the benchmark dunes discussed in Fig. 3 of this letter, the rotation rates were varied and their values can be found in Table S1.

	$\Omega_{\text{table}}$ (rpm)	$\Omega_{\text{paddle}}$ (rpm)	$\Omega_{\text{tot}}$ (rpm)
Benchmark 1	-4.0	7.5	11.5
Benchmark 2	-4.1	7.7	11.8
Benchmark 3	-4.2	7.9	12.1
Benchmark 4	-4.3	8.1	12.4
Benchmark 5	-4.4	8.3	12.7
Benchmark 6	-4.5	8.5	13.0

Table S1. Rotation rates for the benchmark dunes

## DUNE MORPHOLOGY

Table S2 presents some geometric parameters of the dunes in our experiments. Definitions of the quantities are explained in Fig. S2. The lengths are reconstructed from the videos and are measured along the outer wall of the channel.

Dune	Time	L (cm)	H (cm)	Stoss slope (°)	Lee slope (°)
Up	5' ± 2'	51.4 ± 1.9	5.8 ± 0.1	8.3 ± 1.1	19.8 ± 3.6
Up	78' ± 2	50.5 ± 2.1	6.0 ± 0.2	9.1 ± 0.7	19.9 ± 2.69
Down	5' ± 2'	42.1 ± 2.7	6.3 ± 0.2	13.5 ± 1.5	19.8 ± 3.2
Down	78' ± 2'	48.8 ± 1.3	5.8 ± 0.1	9.4 ± 1.3	19.8 ± 3.4

Table S2. Dune geometry

## MEASUREMENT TECHNIQUES

The most important experimentally measured quantities of the letter are

1. Dune migration speed  $c$
2. Dune length  $L$
3. Azimuthal flow speed  $\bar{u}$
4. Mobile layer  $\phi$ .

The first two of them are inferred from the continuous video recording, while the flow speed was estimated using particle tracking in short videos. The last quantity was calculated using recording by a co-rotating camera. We now discuss each of these techniques in sequence.

### Continuous recording

Continuous bed imaging makes use of a stationary Camera B, recording at 200 Hz, aimed at the flume's central axis. The cylindrical LED panel inside the annulus provides the appropriate back-lighting. Camera B is focused on a narrow interrogation window (c.a. 170 mm x

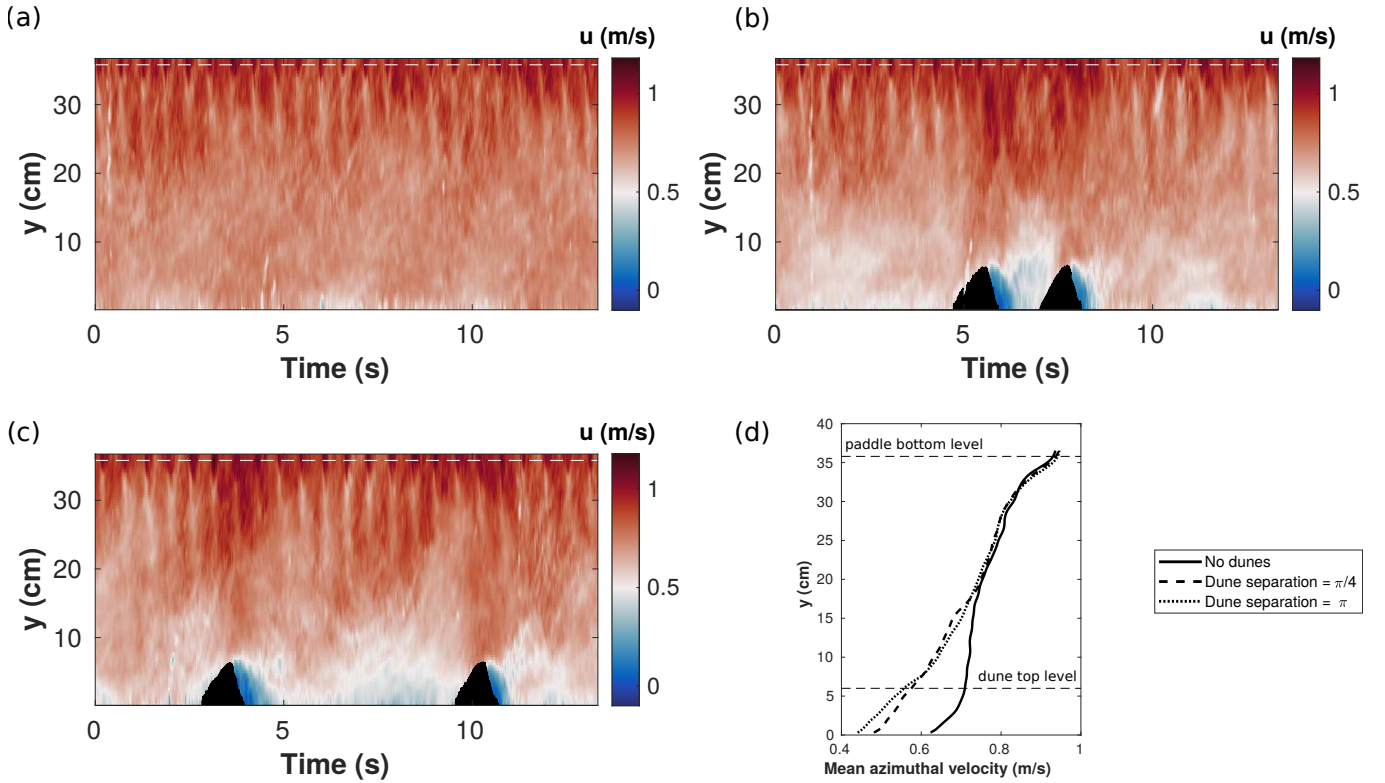


Figure S1. (a) Time course of instantaneous azimuthal velocity in empty tank with driving speed corresponding to Benchmark 6. (b) Time course of instantaneous azimuthal velocity for two dunes in close proximity (angular separation  $\frac{\pi}{4}$ ). (c) Time course of instantaneous azimuthal velocity for two dunes in an antipodal position (angular separation  $\pi$ ). (d) Time-averaged azimuthal velocity for the data from panels a-c (regions corresponding to dunes are excluded).

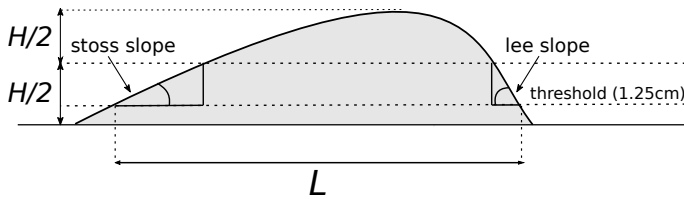


Figure S2. Schematic explaining the definitions of quantities in Table S2.

3 mm), but as the system rotates, every point along the circumference appears periodically in the field of view. We identify the position of the water-sediment interface at the centre of each frame by a light intensity threshold. In order to use this approach, we make a simplifying, yet not unreasonable, assumption that bedforms are 2D, i.e. level across the channel. The output consists of a time series  $h(t)$  and by choosing appropriate thresholds, we use it to identify the position of dunes and their lengths at subsequent times. Because every dune appears quasi-periodically in the field of view, we can also infer their migration speed.

### Benchmark

The migration speed and length of benchmark dunes were assessed using 5 minute long continuous recordings. The dune velocity was assessed by measuring the distance travelled by the dune during a fixed time unit. The dune length was measured at every revolution of the table and the error bars on length represent standard deviation within the 5 minutes.

### Separation

We repeated the separation experiment (Fig. 1 of the letter) 10 times. Each experiment lasted 83 minutes which corresponds to 370 rotations of the table. By identifying the position of the dune at each rotation, we compute momentary velocity of the dune between any two rotations. Subsequently, we average these velocities across the 10 experiments and fit a second-order polynomial in time. As the experiments are highly reproducible, this interpolation allows us to create a look-up table for the migration rate of the upstream and the downstream dune. For example, when we use Camera A we cannot measure dune migration rate at

the same time, but we can note the time and infer the migration rate by using the look-up table. Dune lengths presented in Figure 3d originate from the same 10 experiments. Each data point presents an average over 5 consecutive table rotations, but unlike velocities, the length values are presented without any fitting.

### Flow imaging

Flow velocity is measured by tracking neutrally-buoyant pliolite tracer particles. The motion of these particle is recorded with a high-speed camera recording at 2000 Hz. The field of view of this camera is approximately 8 cm wide and 40 cm high. Instantaneous velocity field was constructed from the video footage using Particle Tracking Velocimetry (PTV) module in software *Digiflow*<sup>1</sup> by averaging over 25 consecutive frames using Gaussian coarse-graining. The reference flow speed is defined as a spatiotemporal average over a neighbourhood of a dune defined in Figure 3e. The average is spatiotemporal rather than spatial because the table was rotating and at each point in the domain, flow velocity was measured at a different time.

### Benchmark

Each of the benchmark dunes was imaged ten times using this technique. Figure 3c presents the ensemble average and the errorbars represent standard deviation.

### Separation

Due to the technical limitations of the high speed camera, after taking one video, one has to wait a few minutes before a next one can be recorded. Therefore, to ensure a dense time coverage, the datapoints in Fig. 3c were collected throughout 6 different repetitions of the separation experiment.

### Co-rotating camera

Type A camera is mounted to the turntable 7 cm away from the outer wall of the flume and its field of view is approximately 4.6 cm high and 20.4 cm wide. Four identical camera stands are available around the table, which allows us to move the camera in the course of one experiment. Each time a dune migrates across the field of

view one video is captured. Camera A uses RGB scale, but only consider the greyscale light intensity  $I$  which we define as an average over the three color channels. In order to quantify the character of sediment transport we analyse the video footage as follows. Firstly, for each frame of the raw image, baseline intensity  $I_0$  is estimated by averaging across the top of the image which is fully lit.  $I_0$  changes over time as the camera dynamically adapts the aperture. Secondly, we compute  $\phi$  by computing the number of pixels where the light intensity laid between  $I_{\text{low}} = \frac{13}{17}I_0$  and  $I_{\text{high}} = \frac{14}{17}I_0$ . Although these bounds were chosen by using a visual criterion, the qualitative results of Fig. 3b are robust to changes in  $I_{\text{low}}$  and  $I_{\text{high}}$  (Fig. S3). In the statistical analysis we have to choose two more parameters: averaging window of the running average  $m$  and noise threshold  $\phi_0$  below which all the data is ignored. In this work we choose the window  $\bar{\phi}$  to be 500 frames and all data corresponding to  $\bar{\phi} < 0.05$  is ignored, but the results are not sensitive to the choices of these parameter values (Fig. S4).

### Benchmark

For each driving speed we recorded the dune with Camera A five times. Each of these videos allowed us to calculate one value of  $\phi$ . Figure 3b shows the averages of the 5 trials with the error bars corresponding to the standard deviation.

### Separation

The separation experiment was repeated six times. Three times, by moving Camera A between the stands, we followed the upstream dune and three times we followed the downstream dune. One data point, corresponding to the earliest measurement at the upstream dune, which had abnormally high value of  $\sigma$ , has been rejected as an outlier.

## SUPPLEMENTARY VIDEOS

Table S3 describes the Supplementary Videos. Videos 1 and 3, as well as 2 and 4, come from the same experiments. Raw videos are played in real time, but the processed videos are sped up four times.

---

\* kab81@cam.ac.uk

† Author is no longer at the institution.

Video	Dune	Type	Speed	Start Time	End Time
1	upstream	processed	x4	6' 52"	10' 9"
2	downstream	processed	x4	1' 38"	3' 47"
3	upstream	raw (greyscale)	x1	6' 52"	10' 9"
4	downstream	raw (greyscale)	x1	1' 38"	3' 47"

Table S3. Supplementary Videos

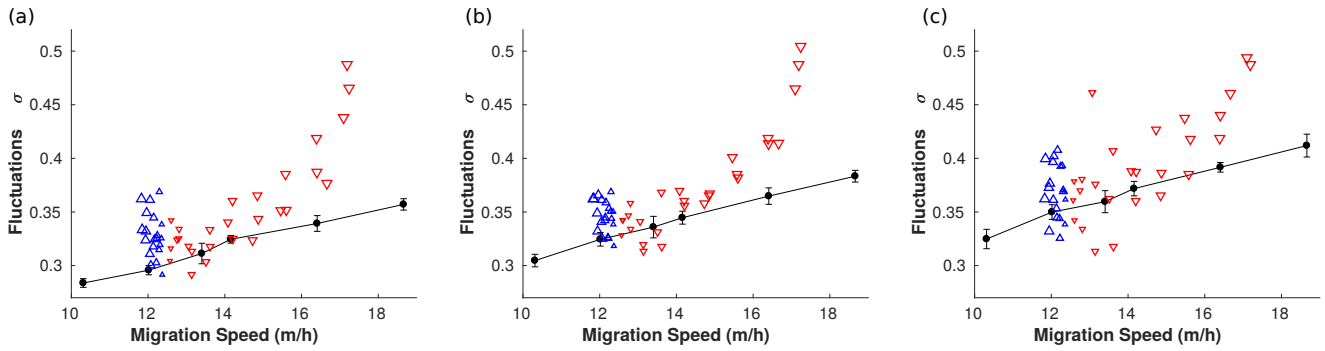


Figure S3. The equivalents of Figure 3b for the different mobile layer thresholds. (a)  $I_{\text{low}} = \frac{12}{17}I_0$ ,  $I_{\text{high}} = \frac{13}{17}I_0$  (b)  $I_{\text{low}} = \frac{13}{17}I_0$ ,  $I_{\text{high}} = \frac{14}{17}I_0$  (used in the letter) (c)  $I_{\text{low}} = \frac{14}{17}I_0$ ,  $I_{\text{high}} = \frac{15}{17}I_0$ .

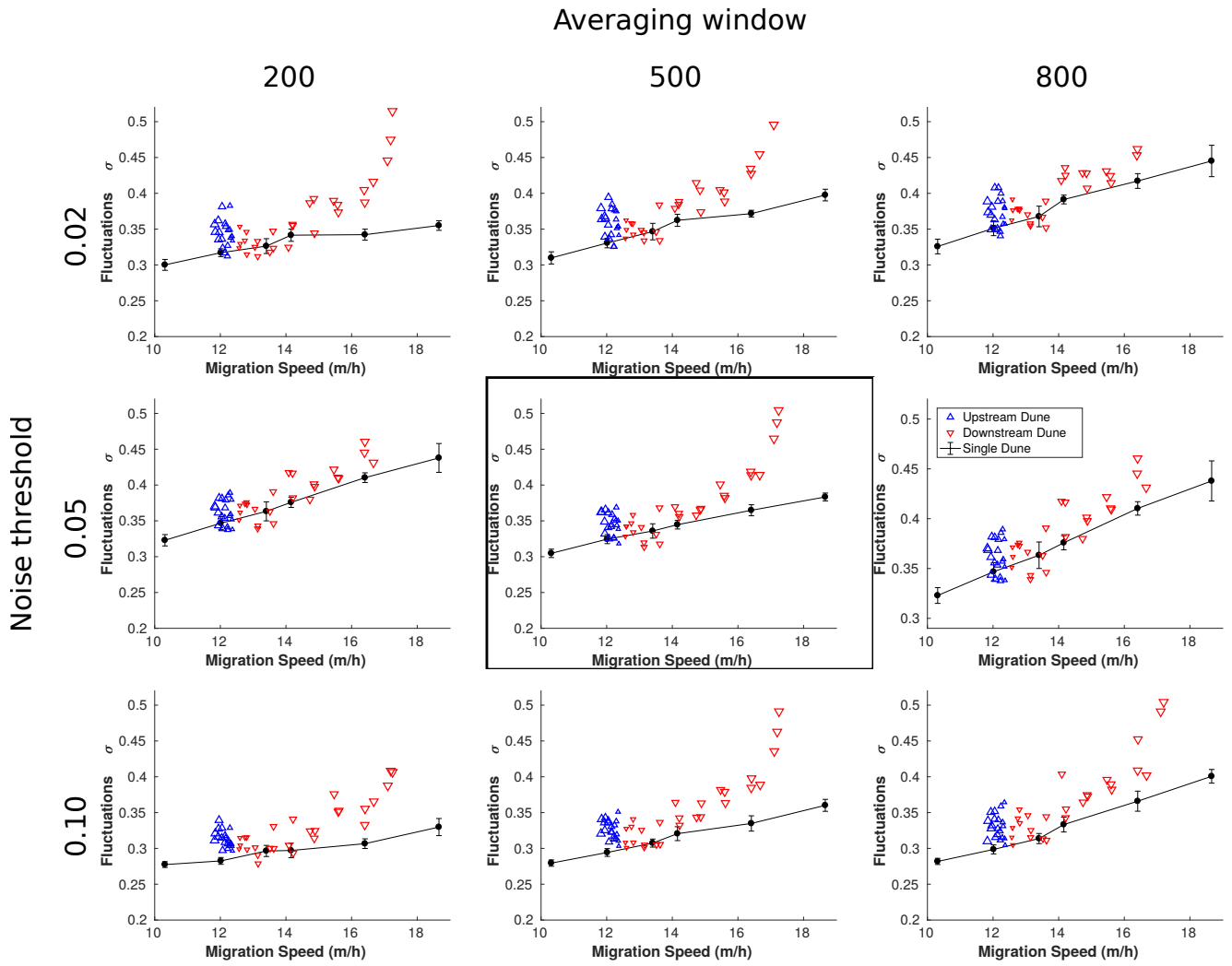


Figure S4. The equivalents of Figure 3b for the different values of the averaging window and noise threshold embedded in the definition of  $\sigma$ . The main results, i.e. elevated fluctuation level for the downstream dune, does not depend sensitively on the choice of these parameters.